Available online at www.sciencedirect.com

ScienceDirect

Procedia CIRP 108 (2022) 654–659

www.elsevier.com/locate/procedia

6th CIRP Conference on Surface Integrity

Machining-induced Surface Integrity in Brass Alloys

Emre Tascioglu[a*], Nima Zoghipour[a,b], Safian Sharif[c], Yusuf Kaynak[b,c]

[a]*Torun Bakır Alaşımları Metal Sanayi ve Ticaret A.Ş., GOSB İhsan Dede Caddesi No: 116 41480 Gebze,Kocaeli, Turkey*

[b]*Department of Mechanical Engineering, Marmara University, 34722 Goztepe Campus-Istanbul,*

[c]*School of Mechanical Engineering, Universiti Teknologi Malaysia, 81310 Johor Bahru, Johor, Malaysia*

* Corresponding author. Tel.: +90 262 677 15; fax: +90 262 677 15 15. *E-mail address:* emre.tascioglu@torunmetal.com

Abstract

This study presents machining process and resulting surface integrity properties of brass alloys including leaded (CW617N), low-leaded (CW511L) and lead-free (CW724R). Experimental data on cutting forces and cutting temperatures are presented to assess machining of these alloys. Surface quality, subsurface microhardness and microstructures of machined brass alloys are considered to assess surface integrity properties. Higher subsurface deformation was observed in low-leaded and lead-free brass materials compared to leaded brass materials. This present study reveals that machining process results in deformation twinning on the surface and subsurface of specimens. The role of machining parameters on performance measures and surface integrity aspects is also presented in this work. This work illustrates that machining parameters have a notable effect on measured machinability outputs. It should be noted that lead content has a strong influence on surface integrity aspects including microhardness and twinning of machined brass alloys.

Keywords: Brass; machining; surface integrity; twinning

1. Introduction

Having good corrosion and wear resistance, electrical and thermal conductivity, and excellent antibacterial properties make brass alloys to be commonly used in industries, such as electric and electronic, automotive, and sanitary [1]. Most of the copper alloys including all types of brass contain Lead elements in their chemical composition. However, currently, these alloys are permitted to have up to 4 %wt. of Lead element according to the directive on the restrictions of the use of certain hazardous substances, RoHS, and the directive on end-of-life vehicles, ELV, approved by the European parliament and council [2,3]. Since Lead is toxic even at low exposure levels and has been found to have acute and chronic effects on human health plants, animals, and micro-organisms [4]. Nonetheless, as the significance of sustainable production is turning out to be progressively perceived, further administrative activities and restrictions could be anticipated in the future.

Although lead content is not preferred due to its negative effect on human health, from machining point of view, lead content helps machinability of brass alloy by substantially increasing chip breakability [5]. But in the meantime, researchers are trying to come up with optimized cutting parameters and conditions for lead-free and low-lead brass alloys.

Schultheiss et al. [5] focused on evaluating the machinability of leaded CuZn39Pb3 brass as compared to lead-free alternative CuZn21Si3P. An improved understanding of the difference in machinability was obtained by comparing the properties and behavior of these two materials in machining. Amaral et al. [1] investigated the machinability of three different brass alloys (leaded, medium-leaded, and minimally leaded) in external turning process with polycrystalline diamond inserts. They

10.1016/j.procir.2022.04.078

focused on cutting forces, chip morphology, and surface roughness in their study. Their results demonstrated the decrease of machinability with the lead reduction, with higher cutting forces and longer chips. Taha et al. [6] studied the machinability of Pb-free brasses with Si from 1 to 4 %wt., which were prepared using Cu 60/Zn 40 and Cu 80/Si 20 Pb-free master alloys. The machinability of the investigated alloys was tested based on cutting force, tool wear, surface roughness, and chip type. According to their results, increasing the silicon content results in increasing the tool wear by 140%, machined surface roughness by 25%, while the chip type changed from continuous to discontinuous type, and the cutting force was reduced by 50%. Nobel et al. [7] carried out an experimental investigation on the influence of material properties, lead content, and tool design on natural and forced chip formation, flow, and breakage in free orthogonal cutting of brass alloys including CuZn38As, CuZn41.5, CuZn21Si3P as well as lead contents (CuZn41.5 Pb=0.003–0.19 %). Zoghipour et al. [8] presented experimental results of the machining performance of lead-free, low-lead and leaded brass alloys in terms of cutting forces, surface roughness, and burr height during milling operations. Moreover, their study also takes the edge radius of cutting tools into account and its role in machining the performance. Empirical equations were derived to predict the machining behavior for each material. In another work [9], they studied drilling process of hot forged lead-free brass alloys by using a form cutting tool. They investigated the cutting forces, dimensional accuracy, and surface quality of the holes considering the tools with different geometries, feed rates, and rotational speeds on hot forged lead-free brass alloys with various copper content. Furthermore, artificial neural network modelling, and genetic algorithm-based optimization methods have been used to predict and optimize the machining process and related responses.

In this paper, both machining performance measures such as the cutting forces, cutting temperatures, and surface integrity aspects including surface quality surface and sub-surface, microhardness and microstructures have been extensively investigated during external turning of leaded (CW617N), low-leaded (CW511L) and lead-free (CW724R).

2. Methodology

2.1. Materials and experiments

Three different types of brass alloys consisted of leaded CuZn40Pb2 (CW617N), low-lead CuZn38As (CW511L), and lead-free CuZn21Si3P (CW724R) with 35 mm diameter and 250 mm length were used as workpiece in this work. The mechanical properties and chemical composition of the test materials are given in Table 1 and 2. The microstructural and phases of the mentioned materials are shown in Fig. 1. It is seen that CW617N and CW511L are composed of α and β phases, while CW724R is consisted of α, κ and γ. The black spots on the CW617N are illustrative for the existence of Lead element. Kistler dynamometer type 9129AA was deployed in order to measure the cutting forces at a sampling rate of 100 Hz for 25 seconds.

Table 1. Chemical composition of the studied brass alloys [10]

Material		Cu	Zn	Pb	Si	As	P	Sn	Fe	Ni	Al
CW617N	%Max	57.0	Rem.	1.6	-	-	-	-	-	-	-
	%Min	59.0	Rem.	2.5	-	-	-	0.3	0.3	0.3	0.05
CW511L	%Max	61.5	Rem.	-	-	0.02	-	-	-	-	-
	%Min	63.5	Rem.	0.2	-	0.15	-	0.1	0.1	0.3	0.05
CW724R	%Max	75.0	Rem.	-	2.7	-	0.02	-	-	-	-
	%Min	77.0	Rem.	0.09	3.5	-	0.10	0.3	0.3		

Table 2. Mechanical, physical, and microstructural properties of the studied brass alloys [10]

Material	*E*(GPa)	ρ (g/cm^3)	Structure	Machinability
CW617N	96	8.43	α+β	%95
CW511L	100	8.25	α+β	%80
CW724R	100	8.41	α+κ+γ	%40

To accomplish reliable results, two repetitions of tests were performed for each set of the chosen cutting parameters, and the average value of the measured main cutting force was considered in the assessments. The experiment parameters are illustrated in Table 3. Optris PI 400i thermal camera was used.

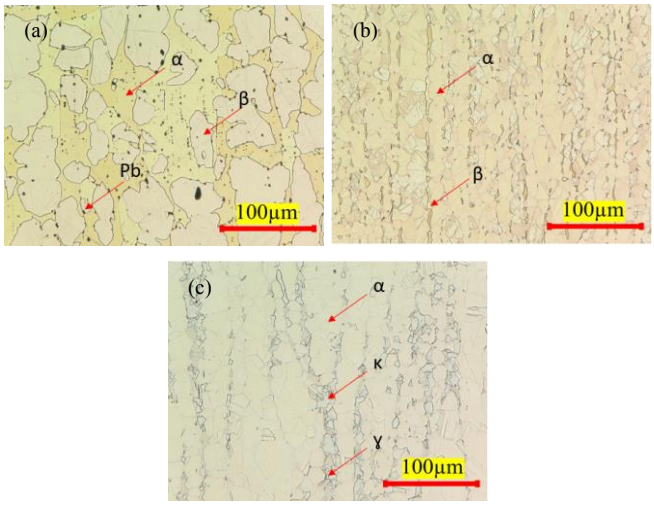

Fig. 1. Microstructure of (a) CW617N; (b) CW511L; (c) CW724R.

The integrity of the machined surfaces was evaluated by Keyence digital optical microscope and SEM (Scanning electron microscope). Optris PI 400i thermal camera was used for measuring the temperature with a rate of 80 frames per second. MHVD 1000 IS microhardness tester was used to measure hardness in accordance with ASTM E 384 standards Micro-hardness tests were performed under 25 g applied load for 10 seconds. Surface roughness evaluations were performed by Mituoyo SV-3000 contracer.

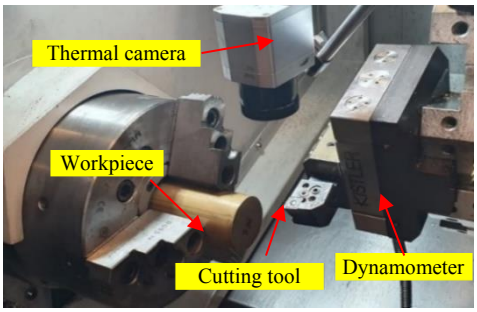

Fig. 2. Experimental setup.

Table 3. The cutting parameters used during the experiments

V_c (m/min)	a_p (mm)	f (mm/rev)	Cutting condition
200	1	0.1 0.15	Dry
400		0.2 0.25	

3. Results and discussion

3.1. Temperature

The temperature measurements during the machining process for the mentioned brass alloys at V_c=200 m/min are presented in Fig. 3. The variation of the temperature of the generated chips arising from the cutting process is illustrated as a function of feed rate and cutting speed in Fig. 4. The temperature was measured for CW511L as 191 °C and 212 °C, whereas the lowest one has been measured for CW617N as 123 °C and 137 °C in 200 m/min and 400 m/min, respectively. It is evident that the generated temperature has been boosted with the increase in feed rate and cutting speed. It is of interest to note that the addition of Lead element is considered as resulting in enhanced machinability through improving the chip breaking [5]. Thermal conductivity values of CW617N, CW511L, and CW724R are 113, 114, and 35 W/(m·K), respectively [10]. The generated chips of CW511L are long and lamellar. CW724R has smaller chips as compared to CW511L. In contrast, the chips of CW617N are discontinuous, short, and easily broken. Although, almost similar thermal conductivity values of leaded and low-lead brasses, the formation of chips has played a major role in the generated temperature on primary and secondary zones of the cut. Long and interbedded chips result in gathering of the material on the tip of the cutting tool and higher temperatures. Therefore, the convenient chip removal process, the more generated temperature is removed.

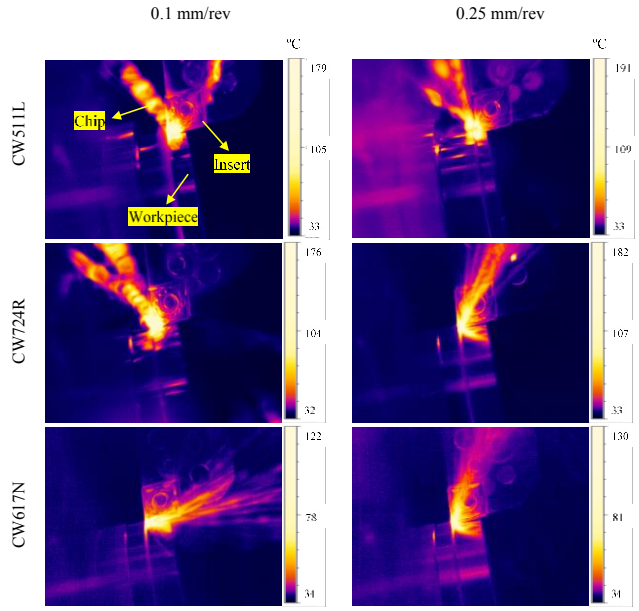

Fig. 3. Temperature measurements during external turning at V_c=200 m/min.

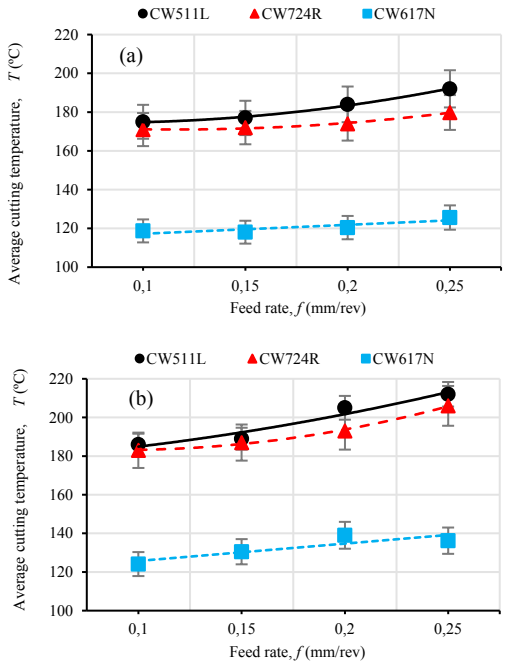

Fig. 4. Average cutting temperature; (a) V_c =200; (b) V_c =400 m/min.

3.2. Cutting Forces

The resultant cutting forces of the mentioned materials are shown in Fig. 5. Average resultant force was observed in machining of CW511L as 396 N and 424 N for cutting speed of 200 and 400 m/min, respectively. However, the lowest values were measured for CW617N as 113 and 126 N. It is clear that the existence of Pb element results in lower cutting forces by keeping more lubricant on its surface helping in the reduction of the wear or friction during the contact.

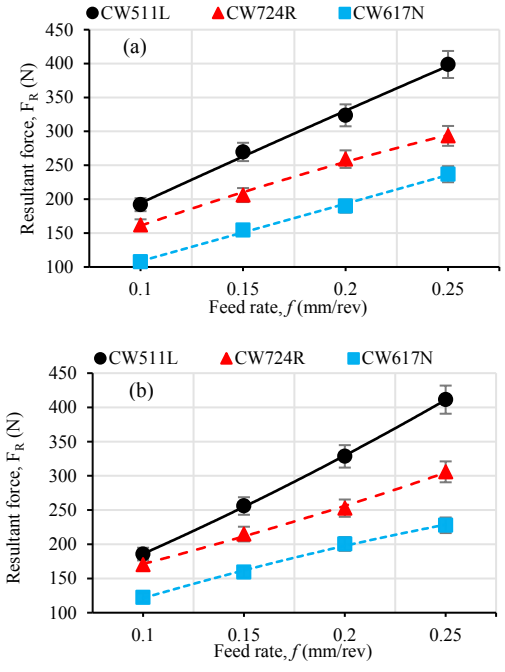

Fig. 5. Average resultant cutting forces; (a) V_c=200; (b) V_c=400 m/min.

Moreover, with the increase of feed rate, the cutting forces have also increased. Notwithstanding the increase in cutting speed, the average resultant forces have not exposed serious variation in terms of the measured value. Furthermore, melting point of CW724R and CW511L are 750 and 900°C, respectively [10]. Therefore, softening during machining can be another reason for the lower cutting forces of CW724R with respect to CW511L. Additionally, this obtained result can be traced back to the silicon-rich κ-phase in the material's microstructure. The κ-phase possesses a higher hardness than the α- and β-phase in silicon-free brasses, and, moreover, it has a BCC lattice structure as confirmation of [7] results.

3.3. Surface roughness

Fig. 6 demonstrates the surface roughness cross-area of the brass alloys with the standard Gaussian filter. The highest value of R_z is measured for CW617N as 10.3 µm at f=0.25 mm/rev and V_c=400 m/min. However, the lowest one is obtained for CW724R as equal to 2.7 µm at f =0.1 mm/rev and V_c=200 m/min. From the figure, it can be deduced that, R_z values of machined surfaces increase with the raise in the Pb element in the alloying composition. In other words, an enhancement on the machined surface is obtained by decreasing the Lead percentage in terms of surface roughness. This can be attributed to the low solubility of Lead and segregation in the entire microstructure and grain boundaries. Moreover, low melting temperature, Tm = 327.5 °C leads to behaving as a lubricant during machining [11]. Furthermore, in spite the feed rate which has affected the R_z value, not a particular variation is observed with the change in cutting speed.

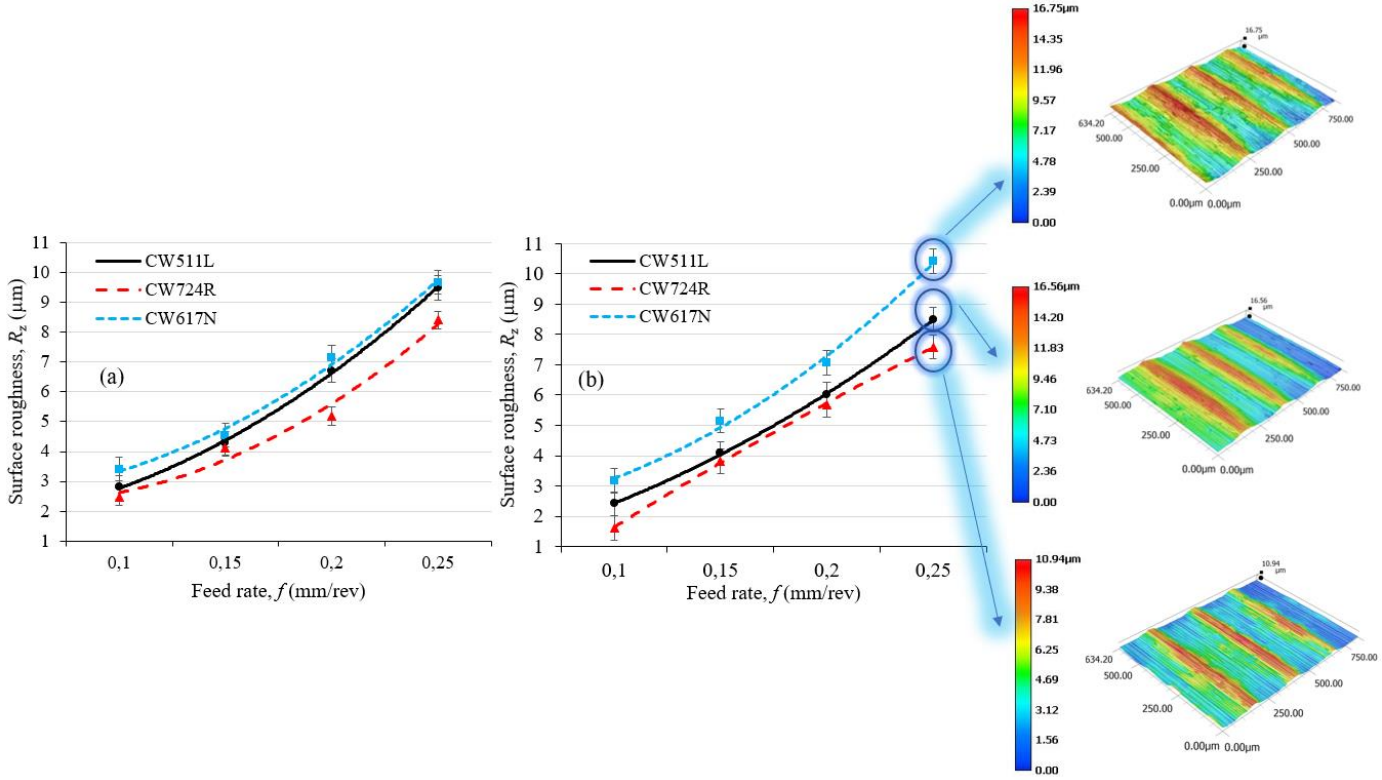

Fig. 6. Surface roughness of machined brass alloys at a) V_c=200 m/min and b) V_c=400 m/min.

3.4. Microhardness

Fig. 7 shows the microhardness variation of the machined sub-surfaces after turning operation. The highest hardness value was measured for the CW724L as 176 and 164 HV for 200 and 400 m/min of cutting speeds, respectively. These values for CW511L were approximately 172, 154, and these were 128, 108 HV for CW617N at 200 and 400 m/min of cutting speeds. It is obvious that the hardness has increased 37%, 84% and 49% as compared to as-received surface for CW617N, CW511L and CW724, respectively. Considering the effect of Pb content on surface and sub-surface hardness variation after machining, notable results are obtained. It should be noted that Pb content play a significant role on hardness increase on machined surface of brass alloy. Indeed, lead content directly impacts on machinability of these materials and thus hardness variation occurs on the machined surface. The higher Pb content, the lower hardness increase resulting from machining. These results show a good correlation with the resulting force results for brass alloys with various Pb content presented in the previous section of this paper. In general, it is observed that hardening occurs in all cutting conditions indicating that the surface of the material experienced intense work hardening achieved by plastic deformation. Furthermore, the hardness of the machined surface increases with the increase of feed rate because of raised contact area between the tool and material and generated

friction and increase of the material flow on the rake face of the tool and its consequences [12]. Increasing feed rate results in increased mechanical work and energy during the cutting process that eventually causes the increased rate of work hardening on the surface and subsurface of the specimen. This is the main reason for the increased hardness on the surface and subsurface of the specimen when machining them with the higher feed rate [12]. But dominant effects on hardness variation comes from Pb content of brass alloy as shown in Fig.7.

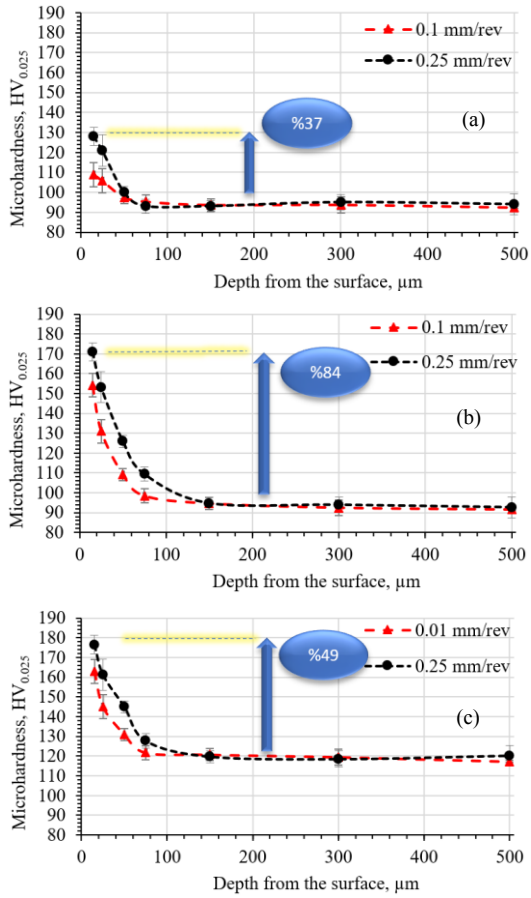

Fig. 7. Measured microhardness; (a) CW617N; (b) CW511L; (c) CW724R.

3.5. Surface and sub-surface microstructure

Fig. 8 represents the SEM images of leaded, low-lead, and lead-free brass alloys. From the images, it can be seen that the surface of all types of brasses has irregularities including hardening of the surface and subsurface along with deformation twinning. The low-lead and lead-free brasses have strong directionality, and their surface is uniform and clearer compared to the leaded brass. In fact, corresponding to the machined surfaces of low-lead and lead-free brass alloys as compared to leaded ones, twinning is being nucleated and the work-hardening is very smooth as an indication of deformation twinning. Further research on the surface and sub-surface deformation and chemical analysis may clarify a brighten hypothesis on the deformation type and shape.

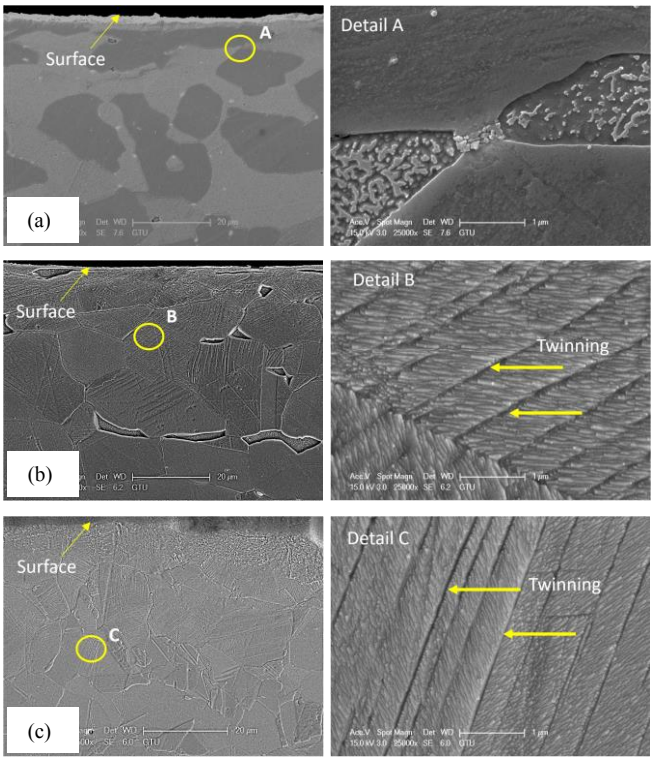

Fig. 8. Surface microstructure; (a) CW617N; (b) CW511L; (c) CW724R.

4. Conclusion

The carried-out research formed fundamental knowledge on the generated temperatures, cutting forces, microhardness, surface and sub-surface microstructure of brass alloys considering the effect of Lead. A significant enhancement in chip breakability and decrease in cutting forces, generated temperature, surface, and sub-surface microhardness is obtained by the existence of Pb. Overall, replacing low-lead and lead-free with leaded brass alloys will bring about higher cutting forces, tool wear, power, and longer chips. In other words, the higher machining cost of the low-lead and lead-free brasses as compared to the leaded brass will be unavoidable.

References

[1] L. Amaral, R. Quinta, T. E Silva, R. MB. Soares, S. D. Castellanos, A. MP. De. Jesus, Effect of lead on the machinability of brass alloys using polycrystalline diamond cutting tools, The Journal of Strain Analysis for Engineering Design, 2018; 53(8): 602-615

[2] J. Buzek, E. Győri, Directive 2011/65/EU on restriction of the use of certain hazardous substances in electrical and electronic equipment. The European Parliment and Council, Strasbourg, 2011.

[3] J.C. Juncker, Commission Directive (EU) 2016/7747 on end-of-life vehicles. European Union, Official Journal of the European Union.2016.

[4] UNEP, Final review of scientific information on lead, United Nations Environment Programme, Chemicals Branch DTIE, 2010.

[5] F. Schultheiss, D. Johansson, V. Bushlya, J. Zhou, K. Nilsson, J. E. Ståhl, Comparative Study on the Machinability of Lead-Free Brass, Journal of Cleaner Production, 2017.

[6] M. A. Taha, N. A. El-Mahallawy, R. M.Hammoud, T. M. Moussa, M. H. Gheith, Machinability characteristics of lead free-silicon brass alloys as correlated with microstructure and mechanical properties. Ain Shams Engineering Journal, 2012; 3(4): 383–392.

[7] C. Nobel, U. Hofmann, F. Klocke1, D. Veselovac, Experimental investigation of chip formation, flow, and breakage in free orthogonal

cutting of copper-zinc alloys, International Journal of Advanced Manufacturing Technologies, 2016; 84:1127–1140.
[8] N. Zoghipour, E. Tascioglu, F. Celik, Y. Kaynak, The influence of edge radius and lead content on machining performance of brass alloys, Procedia CIRP, In press.
[9] N. Zoghipour, G. Atay, Y. Kaynak, Modeling and optimization of drilling operation of lead-free brass alloys considering various cutting tool geometries and copper content, Procedia CIRP, 2021; 102: 246-251.
[10] http:\\www.sarbak.com\document\pdf
[11] K. Aytekin, Characterization of machinability in lead-free brass alloys, KTH Royal institute of technology, Sweden 2018.
[12] N. Zoghipour, E. Tascioglu, G. Atay, Y. Kaynak, Machining-induced surface integrity of holes drilled in lead-free brass alloy, Procedia CIRP, 2020; 87: 148-152.